Density Matrix Embedding: A Simple Alternative to Dynamical Mean-Field Theory

Gerald Knizia and Garnet Kin-Lic Chan

Department of Chemistry, Frick Laboratory, Princeton University, Princeton, New Jersey 08544, USA
(Received 25 April 2012; published 2 November 2012)

We introduce density matrix embedding theory (DMET), a quantum embedding theory for computing frequency-independent quantities, such as ground-state properties, of infinite systems. Like dynamical mean-field theory, DMET maps the bulk interacting system to a simpler impurity model and is exact in the noninteracting and atomic limits. Unlike dynamical mean-field theory, DMET is formulated in terms of the frequency-independent local density matrix, rather than the local Green's function. In addition, it features a finite, algebraically constructible bath of only one bath site per impurity site, with no bath discretization error. Frequency independence and the minimal bath make DMET a computationally simple and efficient method. We test the theory in the one-dimensional and two-dimensional Hubbard models at and away from half filling, and we find that compared to benchmark data, total energies, correlation functions, and metal-insulator transitions are well reproduced, at a tiny computational cost.

Dynamical mean-field theory [1–5] (DMFT) has developed into a powerful embedding framework for bulk quantum systems. Its central idea is to self-consistently map the infinite bulk system to an impurity model, which contains only a few interacting impurity sites, embedded in an infinite noninteracting bath [1–5]. In many settings, such impurity models can be solved using high-level many-body methods (so called impurity solvers) [6–14]. Through the bath embedding, DMFT yields predictions that closely approach the bulk limit, despite the greatly simplified treatment of interactions.

The basic quantum variable in DMFT is the local Green's function, $ig_{ij}(\omega) = \langle a_i^\dagger [\omega - (H - E)]^{-1} a_j \rangle$. As a function of frequency, it provides access to the local density of states as well as to static quantities such as energies. However, there are reasons to consider simpler frequency-independent quantum variables, too. For many applications frequency information is not required; for example, energies can be calculated from time-independent states alone, as can energy derivatives such as compressibilities or static correlation functions, and many other properties. Additionally, calculating stationary states, such as the ground state, is much easier than calculating Green's functions, not the least due to the practical availability of many powerful numerical techniques (e.g., the density matrix renormalization group and its tensor network extensions [15,16], coupled cluster and configuration interaction theories [17], and lattice diffusion [18], auxiliary field [19], and variational Monte Carlo calculations [20,21]). An embedding framework based on a frequency-independent variable offers a potentially more efficient as well as a more flexible route to access static properties of bulk systems, including the possibility of using ground-state methods as impurity solvers.

Here, we propose a density matrix embedding theory (DMET) with the following features: (i) the infinite bulk problem is mapped onto a self-consistent impurity problem, consisting of interacting impurity and noninteracting bath sites, (ii) the single-particle density matrix $\langle a_i^\dagger a_j \rangle$ is the quantum variable, rather than the Green's function, and no frequency-dependent quantities appear in the theory, (iii) the bath representation consists of a single bath site per impurity site (which is sufficient to exactly capture embedding effects at the mean-field level), and (iv) the bath can be constructed algebraically without any fitting. Feature (i) is analogous to DMFT, and as we show below, the basic physics of DMET is similar to DMFT. Features (ii–iv), however, are different. They allow for the primary numerical advantage of DMET: computing ground-state properties of a cluster model with L impurity sites requires only solving for the ground state of a cluster plus bath problem of size $2L$, and this is much cheaper than the corresponding DMFT calculation.

To motivate the DMET construction, we first consider an exact single-site embedding of the infinite lattice Hubbard model, with the Hamiltonian

$$H = \sum_{\langle ij \rangle \sigma} t a_{i\sigma}^\dagger a_{j\sigma} + \sum_i U n_{i\uparrow} n_{i\downarrow}. \tag{1}$$

For simplicity, we focus on ground-state properties, but we outline the extension to excited and thermal states below. The ground state $|\Psi\rangle$ of H can be mapped to the ground state of a simple impurity model, consisting of a single impurity site embedded with a single bath site, and with Hamiltonian H'. This follows from the Schmidt decomposition of $|\Psi\rangle$, $|\Psi\rangle = \sum_i^M \lambda_i |\alpha_i\rangle |\beta_i\rangle$ [22], where $|\alpha_i\rangle$ are states of a single Hubbard site (viewed as an *impurity*) and $|\beta_i\rangle$ are states in the Hilbert space of the remaining lattice sites. Note that the number of $|\beta_i\rangle$ states, M, equals the number of states of the single impurity site. Consequently, $|\beta_i\rangle$ can be interpreted as the states of a single bath site. With this identification, the exact impurity Hamiltonian H'

(with the same ground state as H) may be constructed by projecting H onto the Schmidt basis of impurity and bath states, $H' = \sum_{iji'j'} |\alpha_i \beta_j\rangle\langle\alpha_i \beta_j |H| \alpha_{i'} \beta_{j'}\rangle\langle\alpha_{i'} \beta_{j'}|$. More explicitly, H' can be expressed using the impurity and bath fermionic operators $a^{(\dagger)}$, $b^{(\dagger)}$,

$$H' = c + \sum_\sigma \epsilon_\beta b_\sigma^\dagger b_\sigma + \upsilon(a_\sigma^\dagger b_\sigma + b_\sigma^\dagger a_\sigma)$$
$$+ \sum_{\sigma \neq \sigma'} \upsilon' m_\sigma (a_{\sigma'}^\dagger b_{\sigma'} + b_{\sigma'}^\dagger a_{\sigma'}) + U n_\uparrow n_\downarrow + U_\beta m_\uparrow m_\downarrow,$$
$$(2)$$

where $n_\sigma = a_\sigma^\dagger a_\sigma$, $m_\sigma = b_\sigma^\dagger b_\sigma$, and c, ϵ_β, υ, υ', U_β follow from matrix elements of H with the Schmidt basis, for example, $\upsilon = \langle\alpha_0 \beta_0 |H| \alpha_1 \beta_1\rangle$. Because the impurity Hamiltonian H' has the same ground state $|\Psi\rangle$ as the Hubbard Hamiltonian H, expectation values of the infinite lattice can be obtained exactly from the impurity model. (This is very different from DMFT, where expectation values of the lattice and impurity model are not related in a simple way). For example, the local density matrix is given by $\langle a_\sigma^\dagger a_\sigma\rangle_{H'} \equiv \langle a_{0\sigma}^\dagger a_{0\sigma}\rangle_H$ [the latter referring to lattice sites, Eq. (1)], while the lattice Hubbard energy per site, E, is obtained from the terms in H' which contain the impurity $a^{(\dagger)}$ operator, $E \equiv \langle\sum_\sigma \upsilon(a_\sigma^\dagger b_\sigma + b_\sigma^\dagger a_\sigma) + \sum_{\sigma \neq \sigma'} \upsilon' m_\sigma(a_{\sigma'}^\dagger b_{\sigma'} + b_{\sigma'}^\dagger a_{\sigma'}) + U n_\uparrow n_\downarrow\rangle_{H'}$.

The above construction shows that an impurity model with a single impurity site and a single bath site is in principle sufficient to exactly represent ground-state properties. However, the exact construction is not practically useful: the bath terms in H' require knowledge of the interacting ground state $|\Psi\rangle$ on the infinite lattice and its Schmidt decomposition. The basic idea in DMET is to replace the exact embedding of the Hamiltonian H by one that is exact for a one-particle mean-field lattice Hamiltonian h. The corresponding mean-field embedding bath terms are then easy to compute because the ground state of h is a Slater determinant $|\Phi\rangle$, and its Schmidt decomposition is easily obtained, at a cost no greater than the one-particle diagonalization of h itself [22–24]. As h we choose the one-particle part of H combined with an on-site mean-field interaction operator u (to be determined),

$$h = \sum_{\langle ij\rangle\sigma} t a_{i\sigma}^\dagger a_{j\sigma} + \sum_{i\sigma} u(n_{i\uparrow} + n_{i\downarrow}). \qquad (3)$$

The corresponding DMET impurity Hamiltonian H_{imp} contains a single interacting impurity site, now embedded with a noninteracting bath site,

$$H_{\text{imp}} = \sum_\sigma [\upsilon(a_\sigma^\dagger b_\sigma + b_\sigma^\dagger a_\sigma) + \tilde{u} b_\sigma^\dagger b_\sigma] + U n_\uparrow n_\downarrow. \quad (4)$$

The terms involving the bath operators $b^{(\dagger)}$ in H_{imp} are constructed analogously to the bath terms in Eq. (2), by projecting h onto the Schmidt basis of $|\Phi\rangle$, e.g., given

$|\Phi\rangle = \sum_i^m \lambda_i |\alpha_i\rangle|\beta_i\rangle$, $\upsilon = \langle\alpha_0 \beta_1 |h| \alpha_1 \beta_0\rangle$. Note that the bath terms arising in this way contain only one-particle operators. The mean-field interaction operator u, which defines both the lattice Hamiltonian h and (indirectly) the impurity Hamiltonian H_{imp}, is analogous to the DMFT self-energy. By changing u, we also change the bath terms in H_{imp}, and we can adjust u to obtain a mean-field embedding that *optimally* mimics the exact embedding. One way is to require full self-consistency of the local density matrix, that is, that the mean-field lattice Hamiltonian h and the DMET impurity Hamiltonian H_{imp} yield the same local density matrix: $\langle a_\sigma^\dagger a_\sigma\rangle_{H_{\text{imp}}} = \langle a_{0\sigma}^\dagger a_{0\sigma}\rangle_h$. This is similar to the self-consistency condition on the Green's function in DMFT. We here use a slightly different self-consistency condition, which we have found to be numerically favorable. We minimize the difference between the total density matrices (using both impurity and bath operators) evaluated for the ground states of h and H_{imp},

$$\min_u \sum_{\sigma,c\in\{a,b\}} (\langle c_\sigma^\dagger c_\sigma\rangle_{H_{\text{imp}}} - \langle c_\sigma^\dagger c_\sigma\rangle_h)^2. \qquad (5)$$

This approximately maximizes the overlap between the mean field wave function and the full wave function in the impurity model. Other choices are possible, similar to the different choices of self-consistency condition in DMFT and self-energy functional theories [5,25].

In the exact embedding construction, the impurity Hamiltonian H' and the infinite Hubbard Hamiltonian H shared the same ground state; thus, exact expectation values could be obtained from the impurity model. In the case of the DMET impurity Hamiltonian H_{imp}, this is no longer the case, because the embedding is constructed for the mean-field h rather than H. Nonetheless, in DMET we make the approximation that lattice quantities are approximated by the expectation values of the impurity model. The local density matrix in DMET is thus defined as $\langle a_\sigma^\dagger a_\sigma\rangle_{H_{\text{imp}}}$, and the energy per site is

$$E = \sum_\sigma \upsilon\langle a_\sigma^\dagger b_\sigma + b_\sigma^\dagger a_\sigma\rangle_{H_{\text{imp}}} + U\langle n_\uparrow n_\downarrow\rangle_{H_{\text{imp}}}. \qquad (6)$$

Note that this energy expression is not variational because the embedding in DMET is not exact.

So far we have discussed single-site DMET. Cluster extensions can also be formulated. The simplest cluster extension of DMET for L impurity sites is analogous to L site cellular DMFT [5], and the impurity Hamiltonian H_{imp} is given by

$$H_{\text{imp}} = \sum_\sigma \sum_{i,j=1}^L [\upsilon_{ij}(a_{i\sigma}^\dagger b_{j\sigma} + b_{i\sigma}^\dagger a_{j\sigma}) + \tilde{u}_{ij} b_{i\sigma}^\dagger b_{j\sigma}]$$
$$+ U n_{i\uparrow} n_{i\downarrow}, \qquad (7)$$

where the bath $b_i^{(\dagger)}$, interaction u_{ij}, and coupling υ_{ij} operators are all generalized to L sites. The construction of
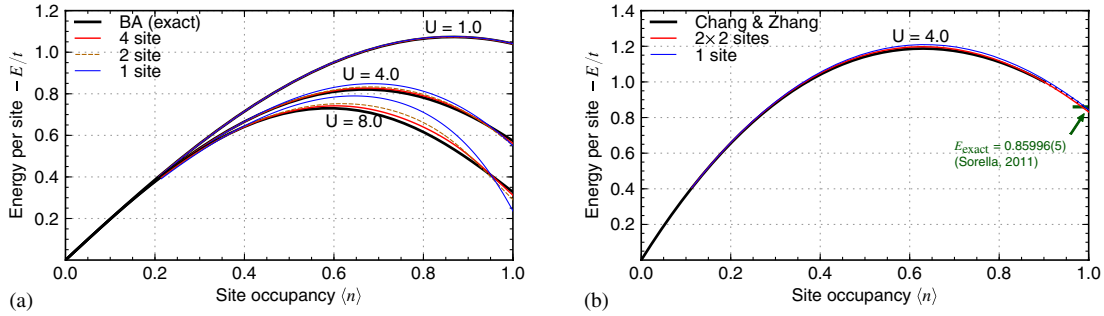
FIG. 1 (color online). $E(n)$ with various cluster sizes: (a) 1D Hubbard model, and (b) 2D Hubbard model. In both cases good agreement with reference data is found. For (b), quantum Monte Carlo reference data are taken from Refs. [28,29].

the couplings from the Schmidt basis of h, the self-consistency conditions on u, and the approximation of lattice quantities by impurity quantities are all directly analogous to the single-site case. Note that this kind of cluster DMET breaks translational invariance, similarly to cellular DMFT [5].

Further extensions are possible, but not followed here. While we have focused on ground states, the DMET construction is equally applicable to excited states (by carrying out the Schmidt decomposition for the excited state, rather than the ground state). In the case of thermal states, we would regard $\exp(-\beta H)$ as a state vector in the enlarged Liouville space to carry out the Schmidt decomposition, leading to impurity and bath sites with twice the number of degrees of freedom as in the case of pure states.

How does DMET perform? Similarly to DMFT, the DMET construction is exact in the noninteracting ($U = 0$) and atomic ($t = 0$) limits of the Hubbard model [3]. In the noninteracting limit, the mean-field lattice Hamiltonian and Hubbard Hamiltonian are the same, $h = H$; thus the mean-field embedding used in DMET is exact. In the atomic limit, the Hubbard Hamiltonian decouples the sites, the impurity-bath coupling $v = 0$ vanishes, and the impurity expectation values are identical to Hubbard model expectation values. DMET thus acts similarly to DMFT in providing an interpolation between metallic and Mott insulating behavior. Note also that DMET has the same diagrammatic structure as DMFT; solution of the impurity Hamiltonian with an exact local interaction ensures that the resulting observables have diagrams where the local interactions are treated to all orders. The different self-consistency condition and bath construction, however, mean that the theories are not identical even in the static limit.

To assess the validity and accuracy of DMET away from exact limits, we now turn to numerical DMET studies of the 1D and 2D Hubbard models, as a function of U and filling. These models were chosen because high-quality reference data are available. In one dimension, we compare to exact results from the Bethe ansatz [26,27], while in two dimensions we compare to recent auxiliary field quantum Monte Carlo calculations [28,29]. In the numerical DMET

calculations, the infinite lattice used to define the mean-field Hamiltonian h in Eq. (3) is approximated by a large lattice with antiperiodic boundary conditions, using 480 sites in the 1D case, and 24×48 sites in the 2D case. The resulting finite size errors are substantially smaller than the intrinsic errors from the DMET approximation. For the DMET impurity solver we employed an exact diagonalization algorithm [30]. The full source code for the prototype DMET and the impurity solver is freely available [24].

We first discuss the ability of DMET to describe energetics and correlation functions in the 1D and 2D Hubbard models. Figure 1 gives the energy per site E, as a function of site occupancy n, using DMET of various cluster sizes. Note that while the 1D Bethe ansatz results are exact, the 2D AFQMC reference data are not [28], except at half filling [29]. As seen from the figure, the overall shapes of the reference $E(n)$ curves are reproduced well. Unsurprisingly, DMET is most accurate at smaller U. The accuracy increases with impurity cluster size, but even single-site DMET produces reasonable energies: at half filling in one dimension, single-site DMET is accurate to 0.12% at $U = 1$, and 4% at $U = 4$, while at half filling in two dimensions, it is accurate to 1.8% at $U = 4$. In Fig. 2 we plot the local double occupancy $\langle n_\uparrow n_\downarrow \rangle$, which is a measure of the Mott insulating character of the state [31].
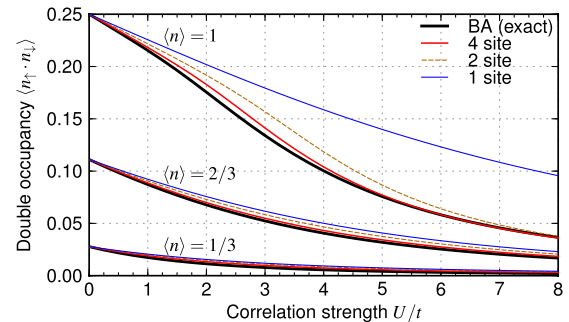

FIG. 2 (color online).   1D Hubbard model: Local double occupancy $\langle n_\uparrow^i \cdot n_\downarrow^i \rangle$ as function of U; at half, 2/6, and 1/6 filling. Except for the 1-site DMET case, the reference shapes are well reproduced.
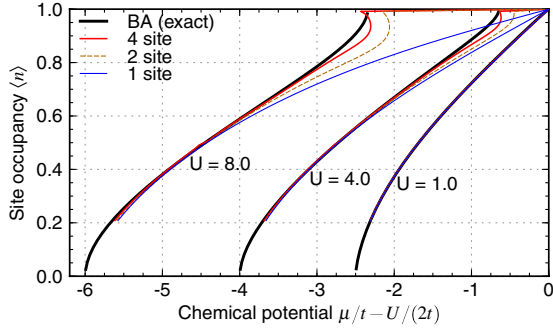
FIG. 3 (color online). Metal-insulator transition in the 1D-Hubbard model: a Mott gap is seen for cluster sizes >1. The size of the gap is accurately reproduced.

FIG. 4 (color online). Comparison of DMET and DMFT descriptions of the metal-insulator transition. DMFT data are taken from Ref. [36].

DMET also gives a good description of this quantity, although at half filling, single-site DMET does not capture the correct change in curvature of $\langle n_\uparrow n_\downarrow \rangle$ as a function of U due to the neglect of short-range singlet formation, while larger clusters recover this interaction effect.

A central question in the DMFT treatment of the 1D and 2D Hubbard models is the location and nature of the metal-insulator transition and the corresponding size of the Mott gap [32–34]. In the antiferromagnetic DMFT solution a gap opens at $U = 0$ due to perfect nesting. The paramagnetic DMFT solution is more complicated, and there is a critical interaction strength U, which depends on the cluster size, beyond which a Mott insulator paramagnetic solution is stabilized. In a ground-state calculation, the opening of a Mott gap can be detected by a vanishing compressibility, $d\langle n \rangle/d\mu$. In Fig. 3 we plot $\langle n \rangle$ against μ for DMET calculations on the 1D Hubbard model. In the antiferromagnetic DMET calculations, a gap opens at $U = 0$ as in DMFT. In the paramagnetic DMET calculations, a Mott transition is observed in the cluster DMET calculations for larger U's, although not in the single-site DMET. Note that single-site DMFT also does not display a Mott transition at moderate U [35]. Compared to the Bethe ansatz, the Mott gap is well reproduced, with the error decreasing with cluster size. The $n(\mu)$ behavior close to half filling shows a bistability, indicating that the metal-insulator transition is likely to be first order, similar to what is found in DMFT. As seen from Fig. 4, the shape of the $n(\mu)$ curves resembles that obtained in recent cellular DMFT studies [35,36]. In the 2D Hubbard model, using a 2×2 cluster DMET, we find coexistence of metallic and insulating paramagnetic solutions over a range of U, in addition to the antiferromagnetic solution (which is correctly identified as the lowest energy phase). The coexistence region starts at about $U \approx 6$ and extends to $U \approx 10.5$. However, the metallic solution is clearly favored up to $U \approx 9.5$ as seen from Fig. 5 (left). Cluster DMET [32,33] and variational plaquette [34] calculations also show a significant coexistence region for paramagnetic metallic and insulating solutions with the
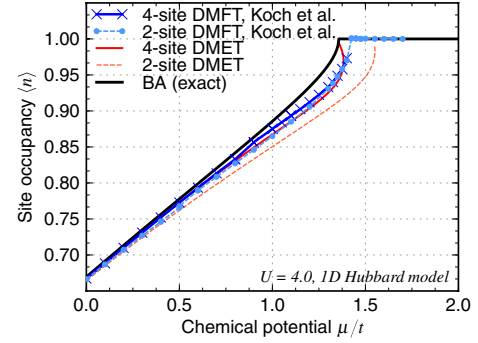
metal-insulator transition occurring near $U \approx 6$. In Fig. 5 (right) we plot $n(\mu)$ for $U = 12$. We see that the structure away from half filling is more complicated than in the 1D plots. Note that this behavior occurs at moderate doping where complex phases of the Hubbard model are expected to exist. Overall, we find that the DMET and DMFT descriptions of the paramagnetic metal-insulator transition are similar, but the DMET calculations of ground-state properties are much cheaper: each one requires computing only the ground state on a very small number of sites, which takes only seconds.

To summarize, here we introduced a density matrix embedding theory to obtain properties of infinite bulk interacting systems from a simpler embedded quantum impurity model. While similar to DMFT, DMET is formulated in terms of the frequency independent local density matrix. The absence of frequency yields both formal and practical advantages. Further, the DMET bath construction requires only a small number of sites (one per impurity), and is obtained algebraically without nonlinear fitting. There is no bath discretization error. The simple bath construction and lack of frequency means that DMET calculations for static properties are much simpler and faster than the corresponding DMFT calculations. We showed that DMET contains similar local physics and is exact in the same limits as DMFT, namely for weak interactions and weak couplings. Furthermore, for the 1D
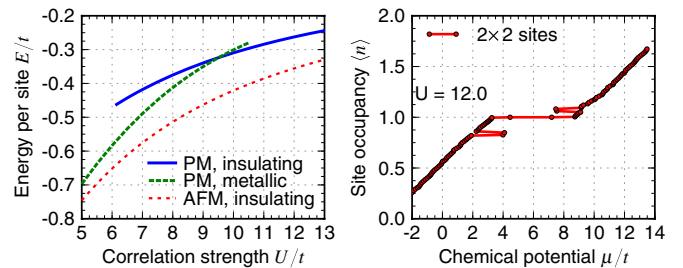

FIG. 5 (color online). 2D Hubbard model. (left) Phase stability of metallic and insulating solutions at half filling as function of U. (right) Paramagnetic metal-insulator transition at $U = 12$.

and 2D Hubbard models, accurate behavior for the energetics, correlations, and metal-insulator transition was observed. Consequently, we conclude that DMET provides an appealing alternative to DMFT for the ground-state properties of infinite interacting systems.

The simplicity of DMET also allows for many extensions. For example, long-range interactions can be considered by projecting the full interacting Hamiltonian into the embedding basis instead of using Eq. (4); initial tests on chemical model systems show excellent results and will be presented elsewhere [37]. Applications to further problems are now underway.

[1] W. Metzner and D. Vollhardt, Phys. Rev. Lett. **62,** 324 (1989).
[2] A. Georges and W. Krauth, Phys. Rev. Lett. **69,** 1240 (1992).
[3] A. Georges, G. Kotliar, W. Krauth, and M. J. Rozenberg, Rev. Mod. Phys. **68,** 13 (1996).
[4] G. Kotliar, S. Savrasov, K. Haule, V. Oudovenko, O. Parcollet, and C. Marianetti, Rev. Mod. Phys. **78,** 865 (2006).
[5] T. Maier, M. Jarrell, T. Pruschke, and M. H. Hettler, Rev. Mod. Phys. **77,** 1027 (2005).
[6] E. Gull, A. J. Millis, A. I. Lichtenstein, A. N. Rubtsov, M. Troyer, and P. Werner, Rev. Mod. Phys. **83,** 349 (2011).
[7] R. Bulla, A. C. Hewson, and T. Pruschke, J. Phys. Condens. Matter **10,** 8365 (1998).
[8] R. Bulla, T. A. Costi, and T. Pruschke, Rev. Mod. Phys. **80,** 395 (2008).
[9] D. J. García, K. Hallberg, and M. J. Rozenberg, Phys. Rev. Lett. **93,** 246403 (2004).
[10] S. Nishimoto, F. Gebhard, and E. Jeckelmann, Physica (Amsterdam) **378B,** 283 (2006).
[11] M. Caffarel and W. Krauth, Phys. Rev. Lett. **72,** 1545 (1994).
[12] H. Hafermann, C. Jung, S. Brener, M. I. Katsnelson, A. N. Rubtsov, and A. I. Lichtenstein, Europhys. Lett. **85,** 27 007 (2009).
[13] D. Zgid and G. K.-L. Chan, J. Chem. Phys. **134,** 094 115 (2011).
[14] D. Zgid, E. Gull, and G. K.-L. Chan, Phys. Rev. B **86,** 165128 (2012).
[15] S. R. White, Phys. Rev. Lett. **69,** 2863 (1992).
[16] F. Verstraete, V. Murg, and J. I. Cirac, Adv. Phys. **57,** 143 (2008).
[17] T. Helgaker, P. Jørgensen, and J. Olsen, *Molecular Electronic-Structure Theory* (Wiley, New York, 2000).
[18] N. Trivedi and D. M. Ceperley, Phys. Rev. B **40,** 2737 (1989).
[19] S. Zhang and H. Krakauer, Phys. Rev. Lett. **90,** 136401 (2003).
[20] S. Sorella, Phys. Rev. B **71,** 241103 (2005).
[21] E. Neuscamman, C. J. Umrigar, and G. K.-L. Chan, Phys. Rev. B **85,** 045103 (2012).
[22] I. Peschel, Braz. J. Phys. **42,** 267 (2012).
[23] I. Klich, J. Phys. A **39,** L85 (2006).
[24] The full source code of the prototype DMET can be obtained at http://www.princeton.edu/chemistry/chan/dmet.
[25] M. Potthoff, Eur. Phys. J. B **32,** 429 (2003).
[26] E. H. Lieb and F. Y. Wu, Phys. Rev. Lett. **20,** 1445 (1968).
[27] H. Shiba, Phys. Rev. B **6,** 930 (1972).
[28] C.-C. Chang and S. Zhang, Phys. Rev. B **78,** 165101 (2008).
[29] S. Sorella, Phys. Rev. B **84,** 241110 (2011).
[30] P. J. Knowles and N. C. Handy, Chem. Phys. Lett. **111,** 315 (1984).
[31] O. Parcollet, G. Biroli, and G. Kotliar, Phys. Rev. Lett. **92,** 226402 (2004).
[32] H. Park, K. Haule, and G. Kotliar, Phys. Rev. Lett. **101,** 186403 (2008).
[33] G. Sordi, K. Haule, and A.-M. S. Tremblay, Phys. Rev. Lett. **104,** 226402 (2010).
[34] M. Balzer, B. Kyung, D. Sénéchal, A.-M. S. Tremblay, and M. Potthoff, Europhys. Lett. **85,** 17 002 (2009).
[35] M. Capone, M. Civelli, S. S. Kancharla, C. Castellani, and G. Kotliar, Phys. Rev. B **69,** 195105 (2004).
[36] E. Koch, G. Sangiovanni, and O. Gunnarsson, Phys. Rev. B **78,** 115102 (2008).
[37] G. Knizia and G. K.-L. Chan (to be published).